LA-5783-MS
Informal Report

C. 3

Implosion, Stability, and Burn of Multishell Fusion Targets

by

Gary S. Fraley
William P. Gula
Dale B. Henderson
Robert L. McCrory
Robert C. Malone
Rodney J. Mason
Richard L. Morse

los alamos
scientific laboratory
of the University of California
LOS ALAMOS, NEW MEXICO 87544

An Affirmative Action/Equal Opportunity Employer

In the interest of prompt distribution, this LAMS report was not edited by the Technical Information staff.

IMPLOSION, STABILITY, AND BURN OF MULTISHELL FUSION TARGETS

by

Gary S. Fraley, William P. Gula, Dale B. Henderson
Robert L. McCrory, Robert C. Malone, Rodney J. Mason, and Richard L. Morse

ABSTRACT

Various multishell laser/e-beam fusion pellets are described. These include a design with hollow fuel inside a high-Z pusher shell which gives greatly improved performance without extreme pulse shaping. The advantage of multishell, multimaterial pellets are discussed in general. Stability calculations then show that Taylor instability on both the inside and outside of shells can amplify perturbations with spherical harmonic ℓ-numbers of the order of 100 by factors exceeding ten thousand. However, by decreasing shell aspect ratios $(r/\Delta r)$ and intensifying the ablation rate these amplifications can be greatly reduced. Acceptable instability growth seems attainable by using aspect ratios of the order of five or less and/or by operating in a less efficient exploding pusher mode. The effects of tamping by high-Z material on thermonuclear burn are briefly discussed.

I. INTRODUCTION

Laser fusion targets generally consist of a spherical pellet, containing fuel and spherical shells of other materials inside of other highly asymmetric structures usually of low-Z materials. The use of a number of contiguous spherical shells of various low-and high-Z materials in laser and e-beam initiated fusion has been under study at the Los Alamos and Livermore Laboratories for many years. The spherical shells serve structural purposes and may improve the implosion. The asymmetric outer structures (see Ref. 1) are designed to absorb and transport energy from one or more laser beams uniformly to the surface of the imploding pellet. In this report studies of the implosion dynamics, the stability, and the thermonuclear burn of multilayered spherical pellets are discussed. Any asymmetric external structure is represented by an outer low-Z portion of the pellet and by assuming spherical illumination.

II. STRUCTURED PELLET IMPLOSION PHENOMENOLOGY

The five simplest pellets are sketched in Fig. 1. Types I and II have been reported in Ref. 2. In Type III the outer low-Z material is usually plastic and improves the symmetry of thermal conduction to the surface of the dense shell. This, or its asymmetric equivalent, is not used in all designs.
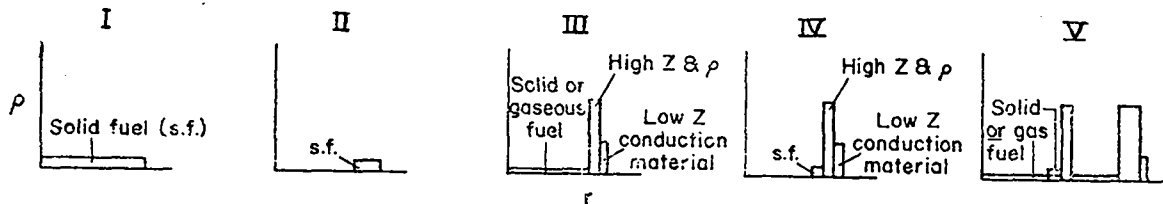

Fig. 1. Five types of laser fusion pellets.

The next layer, or the inner part of it, implodes due to expansion and/or ablation pressure, compressing and heating the fuel. The advantages of this high-Z and ρ pusher/tamper shell, which is in general much more massive than the fuel, are:

1) It provides structural rigidity and containment of initially gaseous fuel at room temperature.

2) The high-Z material shields the fuel from superthermal electron preheat.[3]

3) The higher Z reduces thermal conduction which allows increasing the energy density of implosion without burning through the shell, all other things being equal. Timing of the implosion can be tuned, for a given, usually simple, laser pulse by graduating the Z and ρ of successive layers of shell material.

4) Larger aspect ratio $(r/\Delta r)$ shells accumulate input energy as kinetic energy over a longer implosion time. This allows the use of longer laser pulses with less time tailoring.

5) Kinetic energy imparted to the inside of the pusher shell by outside ablation or by pusher explosion is transferred to the fuel through compression. This becomes important approximately when the fuel pressure exceeds the outside pressure on the shell. With higher initial ρ one has lower specific entropy; this leads to higher ρ of the compressed shell material when energy transfer occurs. Higher shell ρ at this time improves energy transfer and, therefore, compression.

6) Perhaps most important, besides implosion driven by ablation pressure on the outside of the pellet,[2] a pusher shell with much greater initial density than the fuel makes possible the implosion of the fuel by rapid uniform heating of the whole target. The pusher then explodes inward as well as outward. This mode is less efficient but more stable than the ablation mode.

7) High-Z shells are required, because of large scattering rates, for absorption of electrons as well as fuel shielding in e-beam driven fusion.

Type III shells require highly shaped pulses to perform well for the same reasons that bare solid pellets do:[2] strong initial shocking of the fuel precludes high subsequent adiabatic compressions. Lower density gas fillings suffer most because specific entropy increases with decreasing density.

It becomes difficult to keep the fuel from being shocked onto too high an adiabat to allow the needed compressions. Ignition temperatures are much easier to obtain than the necessary compression in these small pellets.

Type IV pellets, in which the fuel is a hollow shell deposited onto the pusher shell (frozen DT or LiDT) are in general far superior to Type III. This hollow type eliminates some of the need of Type III for pulse shaping and makes it possible to achieve ignition values of $\rho R (\gtrsim 0.3 \ g/cm^2)$ with laser energies of $\lesssim 100$ kJ in simple pulse shapes such as Gaussian. The implosion sequence is:

1) The leading tip of the laser pulse sends a weak shock through pusher and fuel, leaving them denser by the shock jump ratio of about four at as little as a few electron volts temperature.

2) Ablation-driven implosion accelerates the pusher shell and fuel inward (except for the ablated material), and further compresses both by this acceleration. In particular, the fuel is kept compressed against the pusher by the effective gravity and assumes an exponential density profile. Increased acceleration adiabatically compresses the fuel and pusher further.

3) Spherical convergence further compresses the fuel and pusher at an increasing rate as the fuel nears the origin.

4) When the tip of the fuel density profile reaches the origin, the density and pressure there rise abruptly and send a shock out from the origin through the fuel. This shock, which increases the fuel density and temperature, reflects between origin and pusher one or two times before becoming negligible.

5) Subsequent fuel compression is adiabatic and continuous until the inner pusher is stopped by fuel pressure. This final compression can increase the fuel density by a factor of about 100 if the pusher specific entropy is low. Acceleration, convergence, and the two shocking steps can contribute another factor of about 100.

6) Because the inner edge of the imploding fuel shell has lower density, this part is more strongly shocked. The resulting sphere of compressed fuel has, therefore, a relatively very hot center which naturally leads to the greater energy efficiency

2

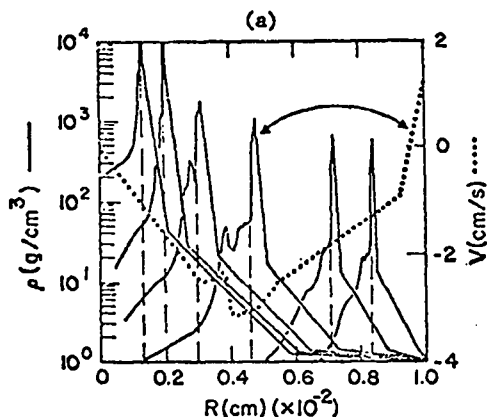obtained from central ignition of thermonuclear burn.[8]

Fig. 2(a). Sequence of density profiles of the 484 μm Type IV pellet absorbing 100 kJ in 3.5 nsec.

Figure 2a is a sequence of spherically symmetric density profiles and one velocity profile from a hollow fuel capsule of initial radius 484 μm with 10 μg of DT fuel (frozen initial ρ = 0.213 g/cm^3), inside of 100 μg of Z = 30, AM = 100, initial ρ = 10 g/cm^3 ideal fluid pusher, imploded by a FWHM τ = 3.5 ns, total energy of E = 100 kJ, Gaussian pulse, showing the inner 100 μm at various times near the end of the implosion and illustrating the points made above. The vertical dashed lines represent the boundary between the pusher and the fuel. At maximum compression the $\int \rho dr$ of the fuel was 0.8 g/cm^2 and of the total pellet was 2.3 g/cm^2, and peak temperature was 10 keV. The initial aspect ratio of the shell was 144.

Improved performance has been achieved from pulse shapes optimized to increase fuel density by increasing inward acceleration just before the fuel reaches center, but such exercises are pointless without the more difficult simultaneous optimization with respect to stability. The pulse may be made shorter and more energetic in order to burn through the pusher during the implosion, thus giving some degree of the exploding pusher behavior described above, to reduce instability. The pusher specific entropy is then greatly increased and the final adiabatic compression is reduced.
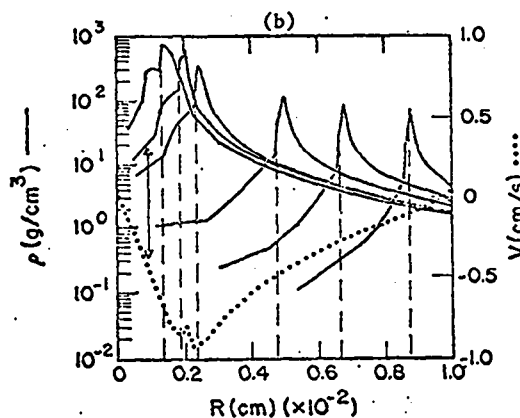

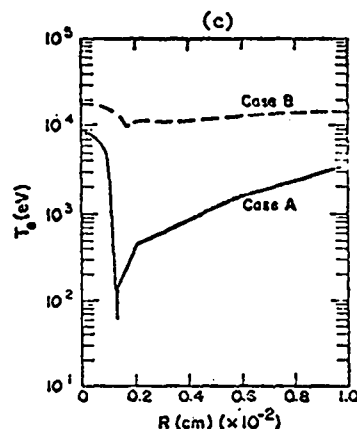Fig. 2(b). An A = 10 pellet absorbing 300 kJ in 400 psec.

Fig. 2(c). The temperature corresponding to the final density profiles in frames (a) and (b).

Figure 2b shows such a case, the same as 2a but with a 0.4 ns, 300-KJ pulse, giving fuel ρR of 0.2 g/cm^2, and total ρR of 0.6 g/cm^2. The hollow fuel capsule had an initial radius of 213 μm, with 2.5 μg of DT fuel frozen inside 100 μg of ideal fluid pusher. The initial aspect ratio of the shell was 10.

Figure 2c shows the electron temperature profiles of the two cases near the time of peak compression. The shorter, more energetic pulse of Case b has eliminated the sharp temperature drop occurring at the fuel-pusher boundary in Case a.

Type V pellets consist of two or more dense shells with masses increasing by about a factor of 10 between successive shells going out from the origin, and with low density, relatively low mass buffer gas in between the shells. This type concentrates energy, i.e., increases energy density, in the fuel through the well-known increase in velocity achieved in elastic collisions between successively smaller masses, but at the expense of considerable inefficiency. Type V (with either a uniform or hollow fuel filling) is suitable for use with e-beam initiation or certain long pulse laser situations where large energies are available, but in which only rather low energy densities can be attained in the outermost shell. This type generally has even more difficulty with instability than the other types discussed.

III. STABILITY

When lower density fuel is being compressed by a much higher density pusher shell near the end of an implosion and the fuel-pusher interface is decelerating, the interface is Taylor unstable.[4] Similarly, the ablation surface on the outside of a shell being accelerated inward by the pressure of lower density ablated material appears to be Taylor unstable, but this case is greatly complicated by thermal conduction in the ablation front and by the continuous flow of material through the ablation surface. However, e-beam imploded shells, in which the ablation involves little thermal conduction, show instability which is similar on the outside and inside. In terms of the ℓ number of spherical harmonic analysis of linear perturbations, when $\ell \gg 1$ the Taylor growth rate at a surface of large relative density discontinuity, at radius r, decelerating at the constant rate a, is:[4]

$$\gamma \simeq \sqrt{\frac{a\ell}{r}} \;, \; \text{or} \; \gamma \Delta t \simeq \sqrt{\frac{2\ell\Delta r}{r}} \qquad (1)$$

after acceleration at a constant rate through a distance Δr for a time Δt. Clearly, since the differential equation for ξ is second order in time, less perturbation amplification occurs if, instead, the acceleration occurs almost impulsively over a smaller fraction of $(\Delta r/r)$, since growth is only linear in time when a = 0, but this is not always

practical. Upper limits on the ℓ number which must be considered are determined by thermal conduction, finite gradient length effects [4] not included in Eq. (1), and by nonlinear saturation effects which are stronger at higher ℓ's (see below).

These observations on Taylor stability of shells seem obvious and have been appreciated since structured laser and e-beam fusion pellets were first considered many years ago. It is not now proper to claim such observations as original.

Recently, a spherical harmonic expansion technique has been developed for obtaining exact solutions of the full first-order perturbation equations based on any heat flow and hydrodynamics process which is spherically symmetric in lowest order.[5] Calculations with this method have shown that the outside surface is stable in a broad class of implosions of Type I targets.[6]

IV. OUTSIDE SURFACE INSTABILITY

Here we report calculations of shell implosions in which there is sufficient inward acceleration to cause significant outside surface instability. These calculations treat simple shells (Type II) but were done with various Z and initial ρ values. These apply, therefore, to Types III, IV, and V. Figure 3 shows the implosion of a Z = 1, AM = 2.5 shell with initial aspect ratio A ≡ (r/Δr), mean radius and density of 20, 850 μm, and 0.2 g/cm³, respectively, with a Gaussian pulse of τ = 2.5 ns, E = 100 kJ, at a time 0.5 ns before peak power.

Figure 3a shows zero order ρ and T; 3b and c show perturbed radial displacement scaled by the amplitude of the initial bumpiness of the outer surface, (ξ_r/ξ_{rI}) for a set of ℓ's covering the range of largest growth. Note that:

1) The ℓ = 50 and 100 results are not incompressible and, in fact, have minima of ξ_r and maxima of $(\bar{\nabla}\cdot\xi_\Omega)$ (not shown) at the unstable surface which are unlike standard Taylor modes. This is either a different, perhaps thermal, instability or a compressibility effect as one should expect at smaller ℓ's.

2) The ℓ = 100 result shows both this compressible structure, near r = 0.062 cm, and a standard Taylor mode structure near 0.064 cm. Higher ℓ's have the pure Taylor form.
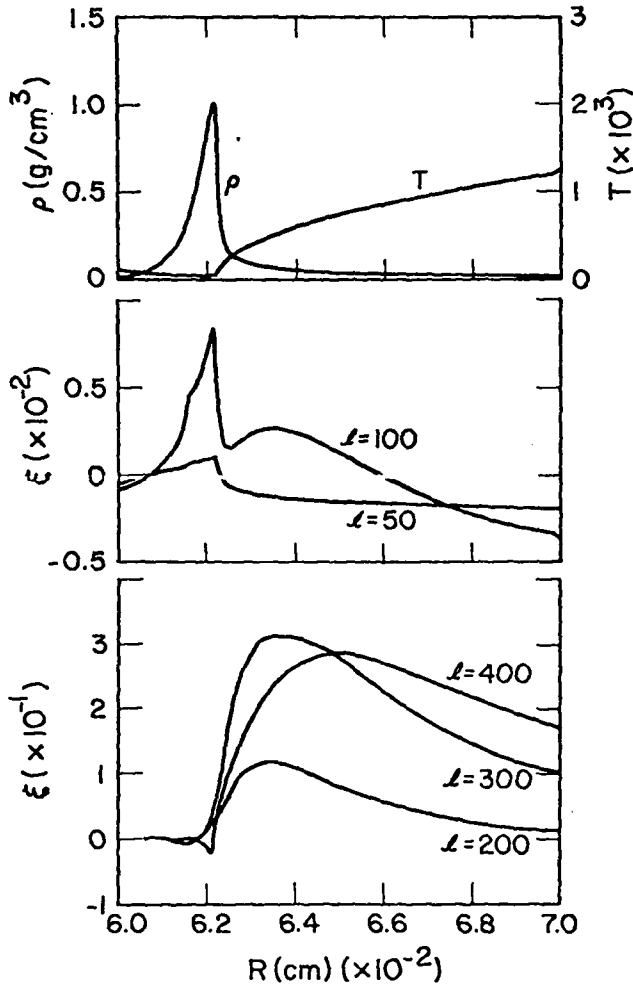
Fig. 3(a). Zeroth order density and temperature
for an A=20 shell. (b) ξ_r (radial dis-
placement) for various ℓ-mode values.
(c) Same as (b).

3) The $\ell \approx 400$ result shows a beginning of re-
versal of the sign ξ near the ablation surface, an
effect which is frequently seen, at high ℓ numbers
first, midway through an implosion.

4) In all cases there is a distinct maximum
of $\xi_r(\ell)$, here at about $\ell = 300$ (see Fig. 5). Pure
Taylor modes without thermal damping would instead
approach a maximum asymptotically with increasing
ℓ as the mode wavelength approached the density
gradient length.[4]

Figure 4 shows growth of $\xi_r(t)$, measured at
the ablation surface, for a value of ℓ near the
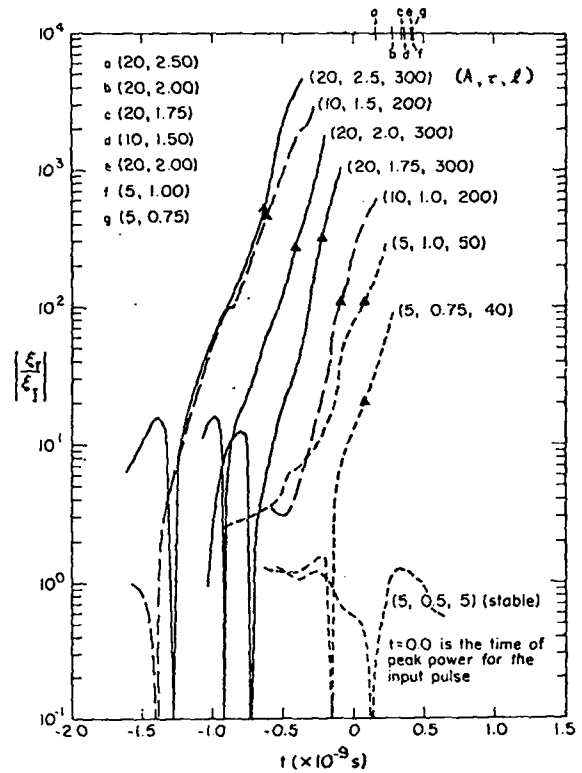maximum for the above case and other cases of the

Fig. 4. Values of ξ_r measured at the ablation
surface for the ℓ-mode of maximum growth
for fixed A and τ.

same Z, ρ, total mass and energy but smaller A and
τ. The times when the insides of the shells touch
the origin are indicated. The smaller τ cases nearly
burn through. Note that the growth is greater for
larger A and τ, and can be 10^4 or greater by the
time the shell touches the center. Total growth is
smaller when (because of smaller r and greater Δr)
τ is smaller and, therefore, the ablation rate and
the temperature at the ablation surface are greater.
Figure 5 shows the spectrum of mode growth of the
various A and τ cases at the times indicated on Fig.
4 by triangles. The local minima correspond to the
mode sign change mentioned above. Growth during the
steeply rising phase (after the sign change, where
it occurs) is consistent with Eq. 1 up to ℓ numbers
at which the angular thermal relaxation rate at the
ablation front (Eq. 9, Ref. 5) is approximately equal
to the Taylor growth rate. It is interesting to
note that during the rapid growth phase (Fig. 4) all
of the exponential growth rates are approximately
the same. Those cases which suffer less total
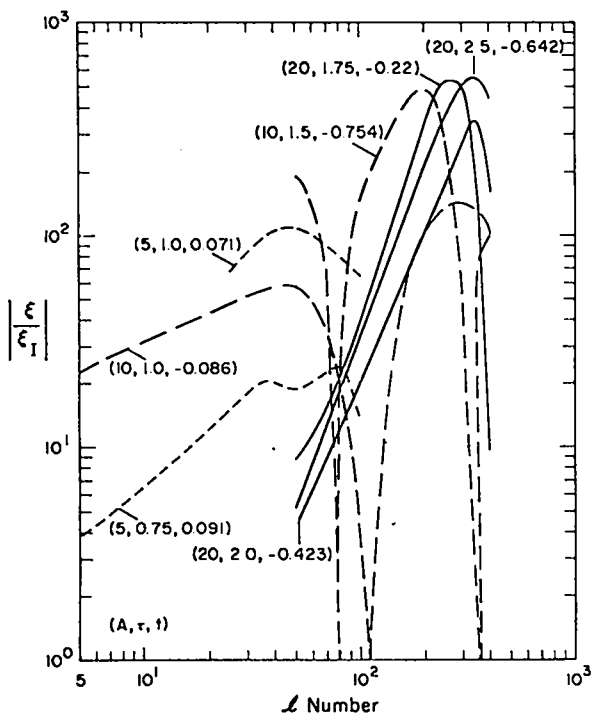growth do so by virtue of a greater delay before

5

Fig. 5. Spectral mode growth of various A and τ cases at the times indicated in Fig. 4.

the beginning of this rapid growth. The ℓ numbers of maximum growth often correspond to mode wavelength of the order of instaneous shell thickness. Higher Z shells with the same mass and A show only slightly smaller growth. It appears that shells with $A > 5$ will be difficult to use except in something close to the uniformly heated, exploding pusher mode (Sec. II above) which further reduces the outside instability growth to virtually nothing in the $\tau \to 0$ limit.

V. INSIDE SURFACE INSTABILITY

Inside instability is reduced by thermal conduction at the higher fuel temperatures of interest. We present here calculations without thermal conductivity, which are more generally scalable and represent the worst case. In our idealized initial conditions the pusher shell has uniform initial density and is in pressure equilibrium with the much lower density fuel. In practice the aspect ratio A is, of course, different from its value at the very beginning of an implosion because of ablation and nonuniform compressions. The initial negative velocity profile is linear throughout the

pusher and everywhere subsonic with respect to the fuel. In practice, compression ratio (and therefore energy transfer efficiency), after fuel pressure has begun decelerating the pusher, increases with the initial ratio of pusher kinetic energy to fuel internal energy and decreases with increasing A in fairly obvious ways.

Figure 6 shows the zero-order density profile of a case in which initially $A = 10$, at a time just before peak compression, together with $\ell = 10$ and 100 values of ξ_r/ξ_{rI} at this time. Initial pusher density and inside radius were 1.0 and 100.0 (arbitrary units); relative initial fuel internal energy and pusher kinetic energy were such as to give a maximum volume compression of $C = 12.8$. Note the familiar exponential form of Taylor modes.
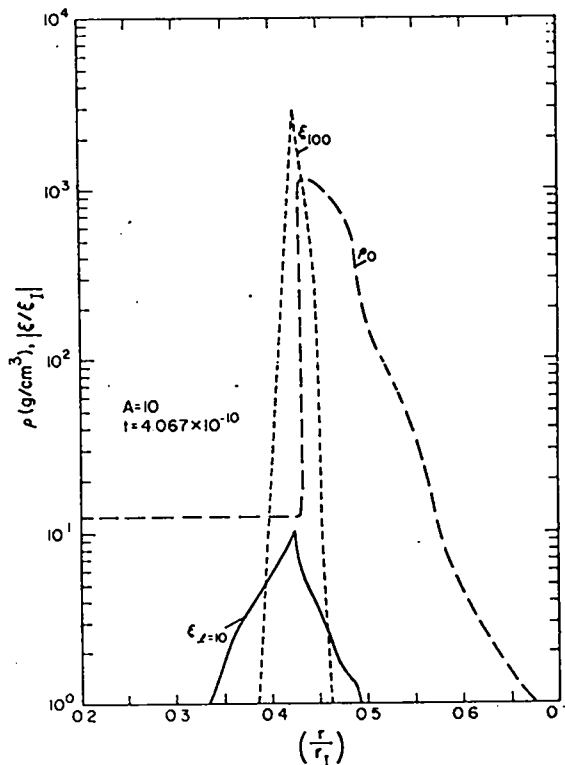

Fig. 6. An $A = 10$ shell inside surface instability just prior to peak compression.

Figure 7 shows the amplitude of various ℓ modes in this case as a function of time. The Fig. 6 points are circled. The time lag before the onset of instability is the time it takes the rarefaction to propagate through the pusher and tell the fuel that
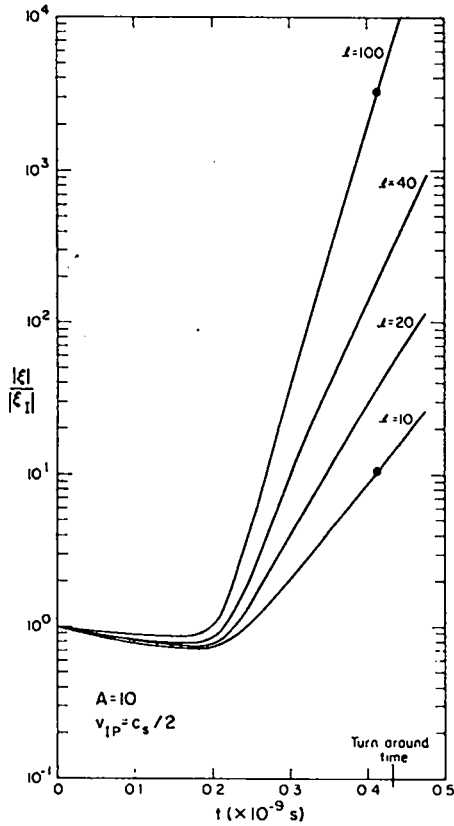
6

Fig. 7. Amplitude of various ℓ modes for an A=10 shell.

Fig. 8. $\ell=100$ mode amplitudes as a function of the pusher inside diameter for various A and C values.

there is no longer anything pushing on the outside of the pusher. This time lag gives some advantage to thicker pushers, as seen in Fig. 8 which shows $\ell = 100$ mode amplitudes as a function of pusher inside diameter for various A and C cases. Clearly, these perturbation growths are large enough to be dangerous.

VI. INSTABILITY DISCUSSION

Regarding linear (small amplitude) growth, note that:

1) The greatest growth of instabilities, in cases of interest, occur at $\ell \gtrsim 20$. Asymmetries introduced by laser irradiation,[5] and probably also e-beams, are damped by thermal conduction between the absorption region and the ablation surface. The asymmetries resulting at the ablation surface are thus limited to $\ell \lesssim 5$. Therefore, instabilities are more likely to be initiated by pellet imperfections than by irradiation asymmetry.
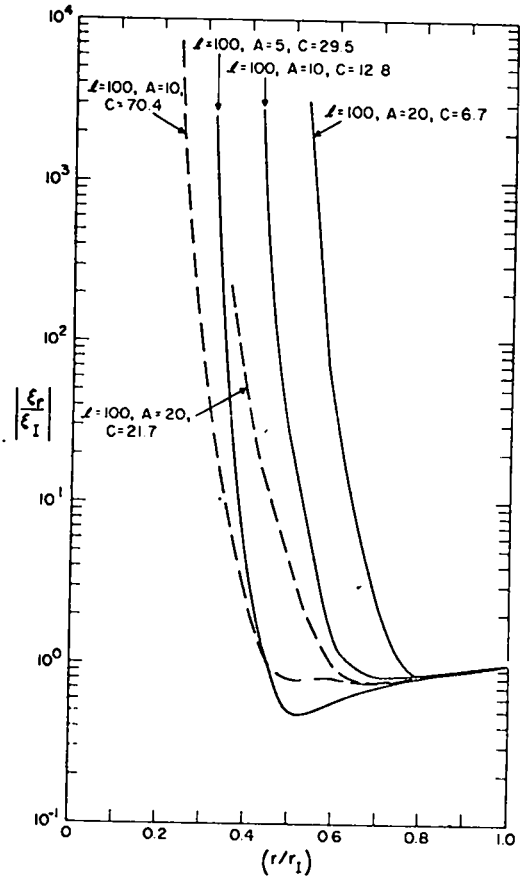
2) Inside growth is large in the ℓ range of maximum growth of outside modes and will, therefore, be initiated by them. However, lower ℓ outside modes are relatively larger on the inside than higher ℓ's and will, therefore, be more effective in initiating inside surface modes than their relative growth at the outside surface would suggest.

3) Inside instability may be reduced by inclusion in pellet design of materials of density intermediate between fuel and pusher to increase the effective density gradient length.

Regarding nonlinear growth, note that:

1) Larger ℓ modes will saturate at smaller amplitudes and will simply mix low-and high-density materials and increase interface gradient lengths without necessarily breaking up a shell. Such mixing might quench the outwardly propagating burn, thus limiting the yield. Reference 7 shows the bubble and spike nonlinear Taylor instability devel-

opment. Details of the nonlinear saturation will depend on the linear mode spectrum, such as shown in Fig. 5.

2) Deeper mixing on the inside, by spike penetration, at smaller ℓ will cool the fuel, limit compression, and prevent or reduce ignition. Outside mixing may modify the implosion by introducing convective heat flow but is not damaging except to the extent that large inside perturbations or even shell breakup are caused.

VII. TAMPED BURN

Studies of thermonuclear burn similar to Ref. 8 but with tamping by high-Z and ρ pusher shell material are reported in Ref. 9. An interesting result of this study is that it is approximately $\int \rho dR$ of fuel and tamper together, not just of fuel, which determines the ignition threshold, as long as the fuel $\rho R > 0.3$ g/cm^2. This can be seen in Fig. 9 which shows the fractional burnup, f_{ro}, for three different fuel masses, tamped with gold where the tamper to fuel density ratio is 4.0 and the mass ratio is 3.0.
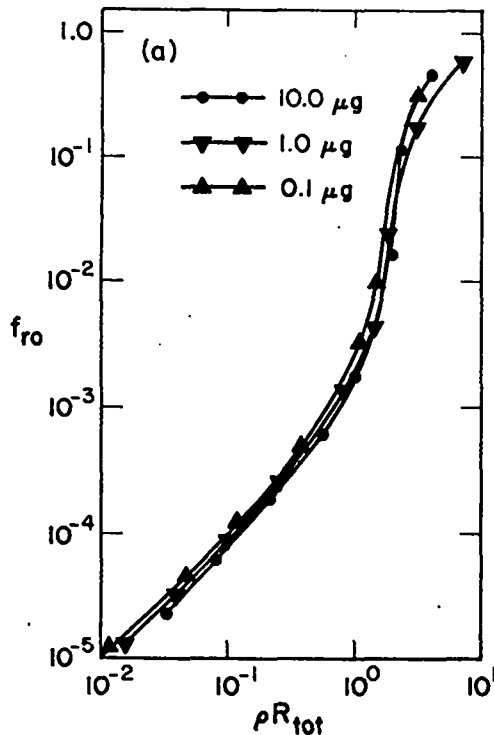

Fig. 9. Burn fraction f_{ro} vs ρR_{tot} for 10, 1, and 0.1 µg of DT, tamped by gold at a mass ratio of 3 and a density ratio of 4 ($=\rho_{Au}/\rho_{DT}$).

REFERENCES

1. G. H. McCall, R. L. Morse, "One Beam Laser Driven Compression Experiments at Los Alamos," Laser Focus (Dec. 1974).

2. J. S. Clarke, H. N. Fisher, R. J. Mason, Bull. Am. Phys. Soc. 17, 1035 (1972); Phys. Rev. Lett. 30, 249 (1973). J. Nuckolls, L. Wood, A. Theissen, G. Zimmerman, Nature, 239 (1972); R. J. Mason, and R. L. Morse, LA-5743-MS.

3. R. L. Morse, C. W. Nielson, Phys. Fluids 16, 909 (1973).

4. S. Chandrasekhar, Hydrodynamics and Hydromagnetic Stability, Ch. X, "The Stability of Superposed Fluids: The Rayleigh-Taylor Instability", Clarendon Press, Oxford (1961).

5. D. B. Henderson, R. L. Morse, Phys. Rev. Lett. 32, 355 (1974).

6. D. B. Henderson, R. L. McCrory, R. L. Morse, Phys. Rev. Lett. 33, 205 (1974).

7. R. H. Harlow, J. E. Welch, Phys. Fluids 9, 842 (1966).

8. G. S. Fraley, E. J. Linnebur, R. J. Mason and R. L. Morse, Phys. Fluids 17, 474 (1974).

9. R. J. Mason, R. L. Morse, "Tamped Thermonuclear Burn of DT Microspheres," Los Alamos Scientific Laboratory Report LA-5789-MS (November 1974).